

Modification of $\chi_{c1}(3872)$ and $\psi(2S)$ Production in p Pb Collisions at $\sqrt{s_{NN}} = 8.16$ TeVR. Aaij *et al.**
(LHCb Collaboration) (Received 22 February 2024; accepted 17 April 2024; published 13 June 2024)

The LHCb Collaboration measures production of the exotic hadron $\chi_{c1}(3872)$ in proton-nucleus collisions for the first time. Comparison with the charmonium state $\psi(2S)$ suggests that the exotic $\chi_{c1}(3872)$ experiences different dynamics in the nuclear medium than conventional hadrons, and comparison with data from proton-proton collisions indicates that the presence of the nucleus may modify $\chi_{c1}(3872)$ production rates. This is the first measurement of the nuclear modification factor of an exotic hadron.

DOI: [10.1103/PhysRevLett.132.242301](https://doi.org/10.1103/PhysRevLett.132.242301)

The study of exotic hadrons with more than three valence quarks is a highly active area of quantum chromodynamics. Dozens of exotic states have been discovered in the last 20 years, and various exotic models such as compact tetraquarks, hadronic molecules, hadrocharmonia, and other structures have been proposed in attempts to explain their various properties (see reviews in Refs. [1–4]). However, to date, there is no general consensus on the nature of the first discovered and most well-studied exotic hadron, the $\chi_{c1}(3872)$ state.

Most existing measurements of the properties of exotic hadrons containing charm quarks utilize their production in the decays of hadrons containing b quarks. These decays provide well-defined initial conditions, and many sources of background can be efficiently rejected using the relatively long lifetime of b hadrons. The LHCb experiment has used these data samples to obtain precise measurements of $\chi_{c1}(3872)$ properties such as its quantum numbers, mass, and width [5–8], and to explore new $\chi_{c1}(3872)$ production channels and decays [9–12]. However, exotic hadrons can also be produced promptly at the interaction point of hadronic collisions, where they can interact with other particles produced in the event. In collisions using beams of nuclei, exotic hadrons can also interact with the nuclear remnant and may be subject to the effects of quark-gluon plasma. The response of the exotic hadrons to these effects provides new ways to constrain their properties, which are not accessible when studying b -hadron decays.

Previous measurements by the LHCb Collaboration in pp collisions showed a significant decrease in the ratio of

prompt $\chi_{c1}(3872)$ to $\psi(2S)$ cross sections, $\sigma^{\chi_{c1}(3872)}/\sigma^{\psi(2S)}$, with increasing charged-particle multiplicity [13]. These data were interpreted in terms of breakup of the $\chi_{c1}(3872)$ hadrons due to interactions with comoving particles produced in the event, for both compact and molecular models of $\chi_{c1}(3872)$ structure [14,15]. The CMS Collaboration has measured the $\sigma^{\chi_{c1}(3872)}/\sigma^{\psi(2S)}$ ratio in PbPb collisions, and found that the ratio is enhanced relative to pp collisions, although that measurement has large uncertainties [16]. Statistical hadronization models predict that $\chi_{c1}(3872)$ production is significantly enhanced in PbPb collisions at the LHC [17,18]. Calculations based on quark coalescence, which can occur when quark wave functions overlap in position and velocity space, show that production rates of $\chi_{c1}(3872)$ hadrons in nucleus-nucleus (AA) collisions are sensitive to its structure. In these models, production of compact tetraquarks is expected to be greatly enhanced over hadronic molecules [19,20], although a recent transport calculation reaches the opposite conclusion [21]. Late-stage interactions in the hadron gas phase of a heavy-ion collision can also affect the observed yields [22]. The suppressing effects of breakup and the enhancing effects of coalescence are expected to dominate in different multiplicity regimes [23], and it is currently unknown where the crossover may occur.

Collisions of protons with Pb nuclei provide an intermediate stage between the relatively small pp collision system and the large PbPb system, and can thereby shed light on the interplay of various enhancement and suppression mechanisms. Calculations of tetraquark production in p Pb collisions have predicted that the $\chi_{c1}(3872)$ cross section could be enhanced relative to pp collisions, due to a higher rate of double-parton scattering [24]. An increase of double-parton scattering in p Pb collisions relative to pp collisions has since been measured by the LHCb Collaboration [25]. An enhancement of proton production relative to pions and kaons has been observed in d Au and p Pb collisions [26–28], which can be explained

*Full author list given at the end of the Letter.

by coalescence of three quarks into baryons versus two quarks into mesons [29–31]. Similarly, an enhancement of charmed baryons relative to charmed mesons has been observed in pp and $p\text{Pb}$ collisions, relative to expectations from e^+e^- collisions [32,33], which may be explained by quark coalescence. These coalescence effects could be even more pronounced for four-quark states, which have not previously been measured in pA collisions. Therefore, in addition to providing novel information on the $\chi_{c1}(3872)$ structure, measurements in $p\text{Pb}$ collisions can provide new tests of models of particle transport and hadronization in nuclear collisions, in a new range of number of constituent quarks.

This Letter describes the first measurements of the prompt production of the exotic state $\chi_{c1}(3872)$ in $p\text{Pb}$ collisions, including the ratio of $\chi_{c1}(3872)$ to $\psi(2S)$ cross sections and the $\chi_{c1}(3872)$ nuclear modification factor $R_{pA}^{\chi_{c1}(3872)}$. The $\chi_{c1}(3872)$ and $\psi(2S)$ hadrons are reconstructed through their decays to $J/\psi\pi^+\pi^-$, where the J/ψ particle subsequently decays to a pair of oppositely charged muons. These measurements use pp and $p\text{Pb}$ collision data recorded by the LHCb experiment. The pp data were collected in 2012 at a center-of-mass energy $\sqrt{s} = 8$ TeV, corresponding to an integrated luminosity of about 2 fb^{-1} . The $p\text{Pb}$ data were collected in 2016 in two configurations. In the forward configuration, denoted $p\text{Pb}$, the proton beam is directed into the LHCb spectrometer and measurements cover the rapidity interval $1.5 < y < 4$, where y is measured in the center-of-mass frame of the proton-nucleus system. In the backward configuration, denoted $\text{Pb}p$, the Pb beam travels into the spectrometer and the resulting rapidity coverage is $-5 < y < -2.5$. The $p\text{Pb}$ and $\text{Pb}p$ datasets considered here were recorded at a center-of-mass energy per nucleon $\sqrt{s_{\text{NN}}} = 8.16$ TeV, and correspond to integrated luminosities of about 12.5 and 19.3 nb^{-1} , respectively.

The LHCb detector is a single-arm forward spectrometer, described in detail in Refs. [34,35]. Events considered in this analysis are selected with a series of triggers which retain events containing the decay $J/\psi \rightarrow \mu^+\mu^-$. The offline selection requires muon candidates to have total momentum $p > 3 \text{ GeV}/c$ and transverse momentum $p_{\text{T}} > 650 \text{ MeV}/c$, and to penetrate hadron absorbers in the muon system. Candidate J/ψ mesons are formed from pairs of oppositely charged muon candidates that have an invariant mass within three standard deviations ($\sim 39 \text{ MeV}/c^2$) of the mean of the J/ψ peak. Charged pion candidates are required to have $p > 3 \text{ GeV}/c$ and $p_{\text{T}} > 500 \text{ MeV}/c$, and are identified by the response of the ring-imaging Cherenkov detectors. Combinations of $\mu^+\mu^-\pi^+\pi^-$ candidates that form a good quality common vertex are retained, and the tracks are refit with kinematic constraints that require all four tracks to originate from a common vertex and constrain the $\mu^+\mu^-$ invariant mass to the known J/ψ mass [36]. The difference between the $J/\psi\pi^-\pi^+$

mass and the sum of the J/ψ and $\pi^+\pi^-$ masses is required to be less than $300 \text{ MeV}/c^2$, which reduces combinatorial backgrounds while retaining signal. The resulting $J/\psi\pi^+\pi^-$ candidates are required to have $p_{\text{T}} > 5 \text{ GeV}/c$.

The $\chi_{c1}(3872)$ and $\psi(2S)$ signals of interest are produced promptly at the collision vertex, where they are subject to interactions with other particles in the event. The pseudo decay-time t_z is used to select promptly produced signal candidates and reject those produced in decays of b hadrons. This variable is defined as

$$t_z \equiv \frac{(z_{\text{decay}} - z_{\text{PV}}) \times M}{p_z}, \quad (1)$$

where $z_{\text{decay}} - z_{\text{PV}}$ is the difference between the positions of the reconstructed vertex of the $J/\psi\pi^+\pi^-$ candidate and the associated collision vertex along the beam axis, M is the mass of the reconstructed signal candidate, and p_z is the candidate's momentum along the beam axis. A requirement of $t_z < 0.1 \text{ ps}$ is applied. The data and simulations show that this retains more than 99% of the prompt signals, while rejecting $\sim 80\%$ of the signals produced in decays of b hadrons. Previous measurements have shown that the fraction of $\chi_{c1}(3872)$ and $\psi(2S)$ that are produced promptly in pp collisions at 8 TeV are about 80% and 75%, respectively [13], and that b hadron production is not significantly modified in $p\text{Pb}$ collisions [37]. Therefore the t_z requirement produces data samples with a highly enriched prompt component and a negligible contribution from b decays. The resulting $J/\psi\pi^+\pi^-$ invariant mass spectra from pp , $p\text{Pb}$, and $\text{Pb}p$ collisions are shown in Fig. 1.

The $J/\psi\pi^+\pi^-$ mass distributions are fit to extract the ratio of $\chi_{c1}(3872)$ to $\psi(2S)$ signal yields. In the fit, the $\chi_{c1}(3872)$ line shape is represented by a Gaussian function, while the $\psi(2S)$ peak is represented by the sum of two Crystal Ball functions, with both low- and high-mass tails [38]. The background is studied by constructing the invariant mass spectrum of $J/\psi\pi^\pm\pi^\pm$ combinations using like-sign dipions, and is well represented by a third-order Chebychev polynomial in all datasets. When fitting the $p\text{Pb}$ and $\text{Pb}p$ samples, the $\chi_{c1}(3872)$ and $\psi(2S)$ line shapes including the $\chi_{c1}(3872)$ mass are fixed to the values determined by fitting the relatively large pp sample, while the $\psi(2S)$ mass, the signal yields, and the background parameters are allowed to float.

The $\chi_{c1}(3872)$ signal yields with their statistical uncertainties are determined to be 129 ± 37 and 71 ± 39 for the $p\text{Pb}$ and $\text{Pb}p$ datasets, respectively. The corresponding $\psi(2S)$ yields are 343 ± 32 and 191 ± 30 for the $p\text{Pb}$ and $\text{Pb}p$ datasets. Fit projections are shown overlaid on the data in Fig. 1. The statistical significance of the $\chi_{c1}(3872)$ signal is estimated by calculating $\sqrt{-2 \ln(\mathcal{L}_B/\mathcal{L}_{S+B})}$, where \mathcal{L}_B and \mathcal{L}_{S+B} are the likelihoods under the background-only and signal-plus-background hypotheses [39]. The resulting

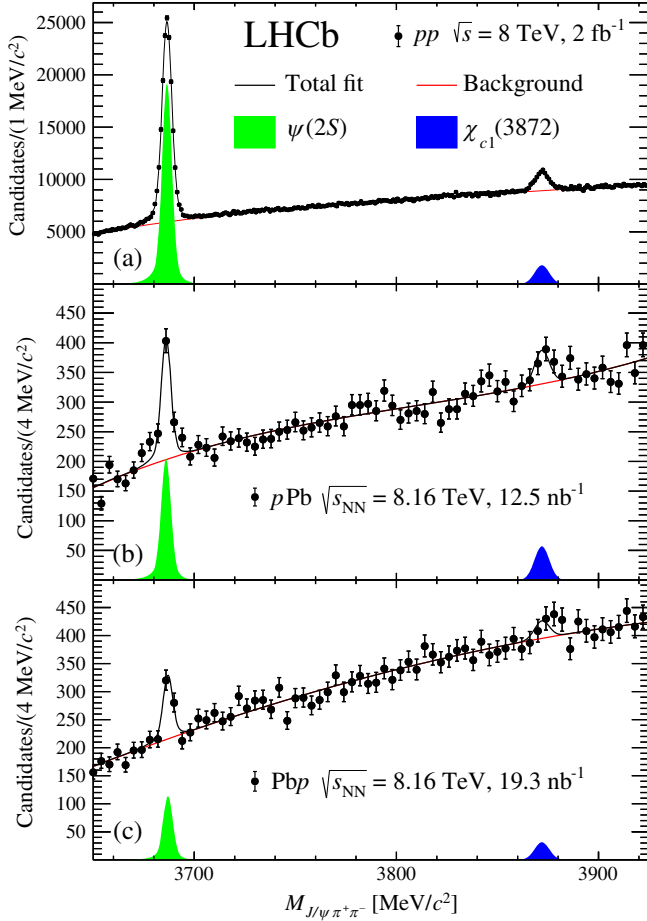


FIG. 1. Invariant mass spectra of $J/\psi\pi^+\pi^-$ candidates measured in (a) pp , (b) $p\text{Pb}$, and (c) $\text{Pb}p$ collisions, with fit projections overlaid.

$\chi_{c1}(3872)$ signal significance is 3.6σ for the $p\text{Pb}$ data and 1.9σ for the $\text{Pb}p$ data. A systematic uncertainty on the fitting procedure is evaluated by changing the $\chi_{c1}(3872)$ fit function to a relativistic Breit-Wigner convolved with a resolution function or a sum of two Crystal Ball functions, and allowing the $\chi_{c1}(3872)$ mass to float. The resulting variation in the ratio of $\chi_{c1}(3872)$ to $\psi(2S)$ signal yields is taken as a systematic uncertainty, which is 5% for the $p\text{Pb}$ data and 27% for the $\text{Pb}p$ data.

Simulation is required to model the effects of the detector acceptance and the imposed selection requirements. In the simulation, $\chi_{c1}(3872)$ and $\psi(2S)$ particles are generated using PYTHIA [40] with a specific LHCb configuration [41], and embedded into the EPOS generator [42], which simulates the environment produced in $p\text{Pb}$ collisions. Decays of unstable particles are described by EvtGen [43]. The interaction of the generated particles with the detector, and its response, are implemented using the GEANT4 toolkit [44] as described in Ref. [45]. The p_T distributions of the simulated $\chi_{c1}(3872)$ and $\psi(2S)$ decays are weighted to match distributions extracted from the data using the *sPlot* method [46] and the results of the fits in Fig. 1.

The ratio of cross sections $\sigma^{\chi_{c1}(3872)}/\sigma^{\psi(2S)}$ times their branching fractions \mathcal{B} to $J/\psi\pi^+\pi^-$ is given by

$$\begin{aligned} & \frac{\sigma^{\chi_{c1}(3872)}}{\sigma^{\psi(2S)}} \times \frac{\mathcal{B}[\chi_{c1}(3872) \rightarrow J/\psi\pi^+\pi^-]}{\mathcal{B}[\psi(2S) \rightarrow J/\psi\pi^+\pi^-]} \\ &= \frac{N_{\chi_{c1}(3872)}}{N_{\psi(2S)}} \times \frac{\epsilon_{\psi(2S)}^{\text{acc}}}{\epsilon_{\chi_{c1}(3872)}^{\text{acc}}} \times \frac{\epsilon_{\psi(2S)}^{\text{trig}}}{\epsilon_{\chi_{c1}(3872)}^{\text{trig}}} \times \frac{\epsilon_{\psi(2S)}^{\text{reco}}}{\epsilon_{\chi_{c1}(3872)}^{\text{reco}}} \\ & \times \left[\frac{\epsilon_{\psi(2S)}^{\mu^{\pm}\text{PID}}}{\epsilon_{\chi_{c1}(3872)}^{\mu^{\pm}\text{PID}}} \right]^2 \times \left[\frac{\epsilon_{\psi(2S)}^{\pi^{\pm}\text{PID}}}{\epsilon_{\chi_{c1}(3872)}^{\pi^{\pm}\text{PID}}} \right]^2, \end{aligned} \quad (2)$$

where $N_{\chi_{c1}(3872)}/N_{\psi(2S)}$ is the ratio of signal yields returned by the fit, and the efficiency ratios are discussed below.

The ratio of LHCb's geometric acceptance for the daughter products $\epsilon_{\psi(2S)}^{\text{acc}}/\epsilon_{\chi_{c1}(3872)}^{\text{acc}}$ is determined from simulation to be close to unity with a systematic uncertainty of 1%, due to the uncertainty on the weights applied to the simulation to match the data. The ratio of trigger efficiencies $\epsilon_{\psi(2S)}^{\text{trig}}/\epsilon_{\chi_{c1}(3872)}^{\text{trig}}$ is determined from data to be consistent with unity within an uncertainty of 2%, using techniques described in Ref. [47], where the uncertainty comes from statistical uncertainties on the data sample. The ratio of reconstruction efficiencies $\epsilon_{\psi(2S)}^{\text{reco}}/\epsilon_{\chi_{c1}(3872)}^{\text{reco}}$ is determined to be 0.67 ± 0.12 (0.61 ± 0.19) for the $p\text{Pb}$ ($\text{Pb}p$) data samples, where the uncertainty is due to the statistical uncertainty on the p_T distributions of signals extracted from the data. The deviation of this term from unity is due to the difference in the kinematics of $\chi_{c1}(3872)$ and $\psi(2S)$ decays. The dipions from $\psi(2S) \rightarrow J/\psi\pi^+\pi^-$ decays have masses between ~ 300 and 600 MeV/c^2 , while the dipions from $\chi_{c1}(3872) \rightarrow J/\psi\pi^+\pi^-$ decays are dominated by intermediate ρ and ω states with higher mass and are reconstructed with a higher efficiency [11]. The ratios of muon and pion particle identification efficiencies, $\epsilon_{\psi(2S)}^{\mu^{\pm}\text{PID}}/\epsilon_{\chi_{c1}(3872)}^{\mu^{\pm}\text{PID}}$ and $\epsilon_{\psi(2S)}^{\pi^{\pm}\text{PID}}/\epsilon_{\chi_{c1}(3872)}^{\pi^{\pm}\text{PID}}$, are determined using calibration samples of identified particles from the data to be consistent with unity, with uncertainties of 1% due to the finite size of those samples [48].

The resulting ratios of fiducial cross sections times branching fractions are $0.26 \pm 0.08 \pm 0.05$ and $0.23 \pm 0.14 \pm 0.10$ in the $p\text{Pb}$ and $\text{Pb}p$ data samples, respectively, where the first and second uncertainties are statistical and systematic, respectively. These ratios are shown in Fig. 2, along with the ratio obtained from multiplicity-integrated LHCb data from pp collisions [13], which has a value of $0.070 \pm 0.009 \pm 0.003$. CMS data from PbPb collisions is also included [16], which is measured over the rapidity interval $|y| < 0.9$ and in a significantly higher p_T range than in the LHCb measurements. In this ratio, some effects that modify charm production in nuclear collisions, such as modification of the nuclear parton distribution function, largely cancel, leaving final-state effects as the dominant

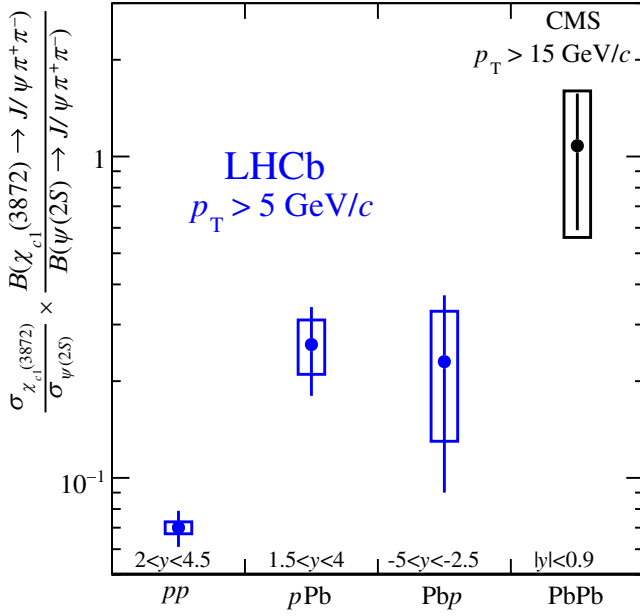


FIG. 2. Ratio of $\chi_{c1}(3872)$ to $\psi(2S)$ cross sections in the $J/\psi\pi^+\pi^-$ decay channel, measured in pp [13], pPb , PbP , and $PbPb$ [16] data. The error bars (boxes) represent the statistical (systematic) uncertainties on the ratio.

modification mechanism. There is an increase in the ratio as the system size increases, which may be due to a combination of effects. It has been observed that $\psi(2S)$ production is suppressed in pA collisions [49–56], which would drive the ratio upwards even if no final-state effects modify $\chi_{c1}(3872)$ production. However, given that pp collisions show a decreasing trend with multiplicity [13], the increase of the ratio may indicate that the hadronic densities achieved in the pPb and PbP configurations allow quark coalescence to become the dominant mechanism affecting $\chi_{c1}(3872)$ production.

This ambiguity between $\psi(2S)$ suppression versus $\chi_{c1}(3872)$ enhancement can be clarified by calculating the nuclear modification factor R_{pPb} . This factor is defined as the cross section σ_{pA} measured in pPb collisions divided by the cross section σ_{pp} measured in pp collisions scaled by the number of nucleons in the nuclear beam, which is 208 for the Pb nuclei used in the LHC. In this case, the ratios of cross sections from pp and pPb collisions shown in Fig. 2, along with the nuclear modification factor of $\psi(2S)$ (measured with relatively high precision in the dimuon channel in Ref. [56]), can be used to find the $\chi_{c1}(3872)$ nuclear modification factor via the equation

$$\begin{aligned}
 R_{pA}^{\chi_{c1}(3872)} &= \frac{\sigma_{pA}^{\chi_{c1}(3872)}}{208 \times \sigma_{pp}^{\chi_{c1}(3872)}} = \frac{1}{208} \frac{\sigma_{pA}^{\chi_{c1}(3872)}}{\sigma_{pp}^{\chi_{c1}(3872)}} \frac{\sigma_{pA}^{\psi(2S)}}{\sigma_{pp}^{\psi(2S)}} \frac{\sigma_{pp}^{\psi(2S)}}{\sigma_{pA}^{\psi(2S)}} \\
 &= R_{pA}^{\psi(2S)} \frac{\sigma_{pA}^{\chi_{c1}(3872)}/\sigma_{pA}^{\psi(2S)}}{\sigma_{pp}^{\chi_{c1}(3872)}/\sigma_{pp}^{\psi(2S)}}. \quad (3)
 \end{aligned}$$

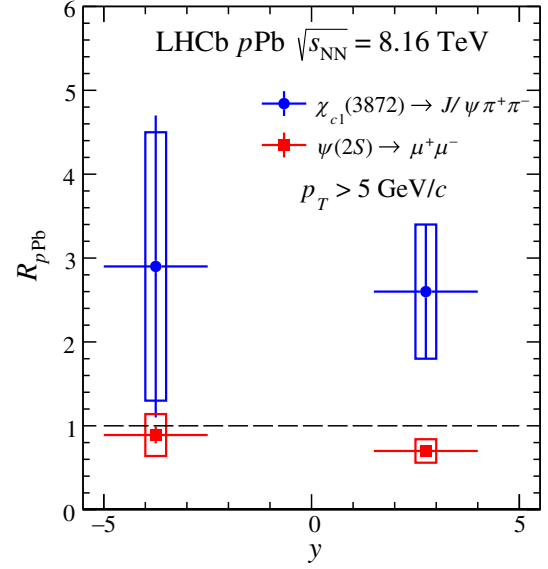


FIG. 3. Nuclear modification factor R_{pPb} for $\chi_{c1}(3872)$ and $\psi(2S)$ hadrons [56]. The error bars (boxes) represent the statistical (systematic) uncertainties.

The resulting nuclear modification factors are $2.6 \pm 0.8 \pm 0.8$ in pPb and $2.9 \pm 1.8 \pm 1.6$ in PbP , where the first and second uncertainties are statistical and systematic, respectively. These results are shown as a function of rapidity in Fig. 3, along with the $\psi(2S)$ measurement from Ref. [56] for comparison. An enhancement of $\chi_{c1}(3872)$ production in pPb collisions as compared to pp collisions is seen, with significant uncertainties. This could indicate that the enhancing effects of coalescence dominate $\chi_{c1}(3872)$ production over the suppressing effects of breakup in pPb collisions. In the compact tetraquark interpretation of the $\chi_{c1}(3872)$ structure, formation via coalescence could occur when a $c\bar{c}$ pair combines with two light quarks. In pPb collisions, the pseudorapidity density of produced charged particles is significantly higher than in pp collisions [57,58], providing an increased probability for quarks to overlap in position and velocity space and potentially coalesce.

In summary, the LHCb Collaboration has produced the first measurements of $\chi_{c1}(3872)$ production in pPb collisions. The increase of the ratio of cross sections $\sigma^{\chi_{c1}(3872)}/\sigma^{\psi(2S)}$ from pp to pPb to PbP collisions may indicate that the exotic $\chi_{c1}(3872)$ hadron experiences different dynamics in the nuclear medium than the conventional charmonium state $\psi(2S)$. The nuclear modification factor R_{pA} shows that production of $\chi_{c1}(3872)$ hadrons in pPb collisions may be enhanced relative to pp collisions, although significant uncertainties preclude drawing firm conclusions. These first measurements of exotic hadron production in pPb collisions can provide new constraints on the allowed configurations of quarks inside hadrons and on models of parton transport and hadronization in nuclear collisions.

We express our gratitude to our colleagues in the CERN accelerator departments for the excellent performance of the LHC. We thank the technical and administrative staff at the LHCb institutes. We acknowledge support from CERN and from the national agencies: CAPES, CNPq, FAPERJ, and FINEP (Brazil); MOST and NSFC (China); CNRS/IN2P3 (France); BMBF, DFG, and MPG (Germany); INFN (Italy); NWO (Netherlands); MNiSW and NCN (Poland); MCID/IFA (Romania); MICINN (Spain); SNSF and SER (Switzerland); NASU (Ukraine); STFC (United Kingdom); DOE NP and NSF (USA). We acknowledge the computing resources that are provided by CERN, IN2P3 (France), KIT and DESY (Germany), INFN (Italy), SURF (Netherlands), PIC (Spain), GridPP (United Kingdom), CSCS (Switzerland), IFIN-HH (Romania), CBPF (Brazil), and Polish WLCG (Poland). We are indebted to the communities behind the multiple open-source software packages on which we depend. Individual groups or members have received support from ARC and ARDC (Australia); Key Research Program of Frontier Sciences of CAS, CAS PIFI, CAS CCEPP, Fundamental Research Funds for the Central Universities, and Sci. & Tech. Program of Guangzhou (China); Minciencias (Colombia); EPLANET, Marie Skłodowska-Curie Actions, ERC and NextGenerationEU (European Union); A*MIDEX, ANR, IPhU, and Labex P2IO, and Région Auvergne-Rhône-Alpes (France); AvH Foundation (Germany); ICSC (Italy); GVA, XuntaGal, GENCAT, Inditex, InTalent and Prog. Atracción Talento, CM (Spain); SRC (Sweden); the Leverhulme Trust, the Royal Society, and UKRI (United Kingdom).

-
- [1] S. L. Olsen, T. Skwarnicki, and D. Zieminska, Nonstandard heavy mesons and baryons: Experimental evidence, *Rev. Mod. Phys.* **90**, 015003 (2018).
- [2] F.-K. Guo, C. Hanhart, U.-G. Meißner, Q. Wang, Q. Zhao, and B.-S. Zou, Hadronic molecules, *Rev. Mod. Phys.* **90**, 015004 (2018); **94**, 029901(E) (2022).
- [3] H.-X. Chen, W. Chen, X. Liu, and S.-L. Zhu, The hidden-charm pentaquark and tetraquark states, *Phys. Rep.* **639**, 1 (2016).
- [4] R. F. Lebed, R. E. Mitchell, and E. S. Swanson, Heavy-quark QCD exotica, *Prog. Part. Nucl. Phys.* **93**, 143 (2017).
- [5] R. Aaij *et al.* (LHCb Collaboration), Determination of the $X(3872)$ meson quantum numbers, *Phys. Rev. Lett.* **110**, 222001 (2013).
- [6] R. Aaij *et al.* (LHCb Collaboration), Quantum numbers of the $X(3872)$ state and orbital angular momentum in its $\rho^0 J/\psi$ decays, *Phys. Rev. D* **92**, 011102(R) (2015).
- [7] R. Aaij *et al.* (LHCb Collaboration), Study of the line shape of the $\chi_{c1}(3872)$ state, *Phys. Rev. D* **102**, 092005 (2020).
- [8] R. Aaij *et al.* (LHCb Collaboration), Study of the $\psi_2(3823)$ and $\chi_{c1}(3872)$ states in $B^+ \rightarrow (J/\psi \pi^+ \pi^-) K^+$ decays, *J. High Energy Phys.* **08** (2020) 123.
- [9] R. Aaij *et al.* (LHCb Collaboration), Evidence for the decay $X(3872) \rightarrow \psi(2S)\gamma$, *Nucl. Phys.* **B886**, 665 (2014).
- [10] R. Aaij *et al.* (LHCb Collaboration), Observation of the $\Lambda_b^0 \rightarrow \chi_{c1}(3872) p K^-$ decay, *J. High Energy Phys.* **09** (2019) 028.
- [11] R. Aaij *et al.* (LHCb Collaboration), Observation of sizeable ω contribution to $\chi_{c1} \rightarrow \pi^+ \pi^- J/\psi$ decays, *Phys. Rev. D* **108**, L011103 (2023).
- [12] R. Aaij *et al.* (LHCb Collaboration), Observation of the $B_s^0 \rightarrow \chi_{c1}(3872) \pi^+ \pi^-$ decay, *J. High Energy Phys.* **07** (2023) 084.
- [13] R. Aaij *et al.* (LHCb Collaboration), Observation of multiplicity-dependent $\chi_{c1}(3872)$ and $\psi(2S)$ production in pp collisions, *Phys. Rev. Lett.* **126**, 092001 (2021).
- [14] A. Esposito, E. G. Ferreira, A. Pilloni, A. D. Polosa, and C. A. Salgado, The nature of $X(3872)$ from high-multiplicity pp collisions, *Eur. Phys. J. C* **81**, 669 (2021).
- [15] E. Braaten, L.-P. He, K. Ingles, and J. Jiang, Production of $X(3872)$ at high multiplicity, *Phys. Rev. D* **103**, L071901 (2021).
- [16] A. M. Sirunyan *et al.* (CMS Collaboration), Evidence for $X(3872)$ in Pb-Pb collisions and studies of its prompt production at $\sqrt{s_{NN}} = 5.02$ TeV, *Phys. Rev. Lett.* **128**, 032001 (2022).
- [17] S. Cho and S. H. Lee, Production of multicharmed hadrons by recombination in heavy ion collisions, *Phys. Rev. C* **101**, 024902 (2020).
- [18] A. Andronic, P. Braun-Munzinger, M. K. Köhler, K. Redlich, and J. Stachel, Transverse momentum distributions of charmonium states with the statistical hadronization model, *Phys. Lett. B* **797**, 134836 (2019).
- [19] S. Cho *et al.* (ExHIC Collaboration), Identifying multiquark hadrons from heavy ion collisions, *Phys. Rev. Lett.* **106**, 212001 (2011).
- [20] S. Cho *et al.* (ExHIC Collaboration), Exotic hadrons in heavy ion collisions, *Phys. Rev. C* **84**, 064910 (2011).
- [21] B. Wu, X. Du, M. Sibila, and R. Rapp, $X(3872)$ transport in heavy-ion collisions, *Eur. Phys. J. A* **57**, 122 (2021); **57**, 314(E) (2021).
- [22] L. M. Abreu, K. P. Khemchandani, A. Martínez Torres, F. S. Navarra, and M. Nielsen, $X(3872)$ production and absorption in a hot hadron gas, *Phys. Lett. B* **761**, 303 (2016).
- [23] Y. Guo *et al.*, Medium-assisted enhancement of $X(3872)$ production from small to large colliding systems, *arXiv*: 2302.03828.
- [24] F. Carvalho and F. S. Navarra, Nuclear effects on tetraquark production by double parton scattering, *EPJ Web Conf.* **137**, 06004 (2017).
- [25] R. Aaij *et al.* (LHCb Collaboration), Observation of enhanced double parton scattering in proton-lead collisions at $\sqrt{s_{NN}} = 8.16$ TeV, *Phys. Rev. Lett.* **125**, 212001 (2020).
- [26] J. Adams *et al.* (STAR Collaboration), Pion, kaon, proton and anti-proton transverse momentum distributions from $p + p$ and $d + Au$ collisions at $\sqrt{s_{NN}} = 200$ GeV, *Phys. Lett. B* **616**, 8 (2005).
- [27] A. Adare *et al.* (PHENIX Collaboration), Spectra and ratios of identified particles in Au + Au and $d + Au$ collisions at $\sqrt{s_{NN}} = 200$ GeV, *Phys. Rev. C* **88**, 024906 (2013).

- [28] J. Adam *et al.* (ALICE Collaboration), Multiplicity dependence of charged pion, kaon, and (anti)proton production at large transverse momentum in p-Pb collisions at $\sqrt{s_{NN}} = 5.02$ TeV, *Phys. Lett. B* **760**, 720 (2016).
- [29] R. C. Hwa and C. B. Yang, Final state interaction as the origin of the Cronin effect, *Phys. Rev. Lett.* **93**, 082302 (2004).
- [30] R. C. Hwa and C. B. Yang, Proton production in $d + Au$ collisions and the Cronin effect, *Phys. Rev. C* **70**, 037901 (2004).
- [31] F.-l. Shao, G.-j. Wang, R.-q. Wang, H.-h. Li, and J. Song, Yield ratios of identified hadrons in $p + p$, $p + Pb$, and $Pb + Pb$ collisions at energies available at the CERN Large Hadron Collider, *Phys. Rev. C* **95**, 064911 (2017).
- [32] S. Acharya *et al.* (ALICE Collaboration), Charm-quark fragmentation fractions and production cross section at midrapidity in pp collisions at the LHC, *Phys. Rev. D* **105**, L011103 (2022).
- [33] S. Acharya *et al.* (ALICE Collaboration), Λ_c^+ production and baryon-to-meson ratios in pp and p-Pb Collisions at $\sqrt{s_{NN}} = 5.02$ TeV at the LHC, *Phys. Rev. Lett.* **127**, 202301 (2021).
- [34] A. A. Alves Jr. *et al.* (LHCb Collaboration), The LHCb detector at the LHC, *J. Instrum.* **3**, S08005 (2008).
- [35] R. Aaij *et al.* (LHCb Collaboration), LHCb detector performance, *Int. J. Mod. Phys. A* **30**, 1530022 (2015).
- [36] R. L. Workman *et al.* (Particle Data Group), Review of particle physics, *Prog. Theor. Exp. Phys.* **2022**, 083C01 (2022).
- [37] R. Aaij *et al.* (LHCb Collaboration), Measurement of B^+ , B^0 and Λ_b^0 production in p Pb collisions at $\sqrt{s_{NN}} = 8.16$ TeV, *Phys. Rev. D* **99**, 052011 (2019).
- [38] J. Gaiser, E. Bloom, F. Bulos, G. Godfrey, C. Kiesling *et al.*, Charmonium spectroscopy from inclusive ψ' and J/ψ radiative decays, *Phys. Rev. D* **34**, 711 (1986).
- [39] S. S. Wilks, The large-sample distribution of the likelihood ratio for testing composite hypotheses, *Ann. Math. Stat.* **9**, 60 (1938).
- [40] T. Sjöstrand, S. Mrenna, and P. Skands, A brief introduction to PYTHIA 8.1, *Comput. Phys. Commun.* **178**, 852 (2008).
- [41] I. Belyaev *et al.*, Handling of the generation of primary events in Gauss, the LHCb simulation framework, *J. Phys. Conf. Ser.* **331**, 032047 (2011).
- [42] T. Pierog, Iu. Karpenko, J. M. Katzy, E. Yatsenko, and K. Werner, EPOS LHC: Test of collective hadronization with data measured at the CERN Large Hadron Collider, *Phys. Rev. C* **92**, 034906 (2015).
- [43] D. J. Lange, The EvtGen particle decay simulation package, *Nucl. Instrum. Methods Phys. Res., Sect. A* **462**, 152 (2001).
- [44] J. Allison *et al.* (GEANT4 Collaboration), GEANT4 developments and applications, *IEEE Trans. Nucl. Sci.* **53**, 270 (2006); S. Agostinelli *et al.* (GEANT4 Collaboration), GEANT4: A simulation toolkit, *Nucl. Instrum. Methods Phys. Res., Sect. A* **506**, 250 (2003).
- [45] M. Clemencic, G. Corti, S. Easo, C. R. Jones, S. Miglioranza, M. Pappagallo, and P. Robbe, The LHCb simulation application, Gauss: Design, evolution and experience, *J. Phys. Conf. Ser.* **331**, 032023 (2011).
- [46] M. Pivk and F. R. Le Diberder, SPlot: A statistical tool to unfold data distributions, *Nucl. Instrum. Methods Phys. Res., Sect. A* **555**, 356 (2005).
- [47] S. Tolk, J. Albrecht, F. Dettori, and A. Pellegrino, Data driven trigger efficiency determination at LHCb, CERN, Report No. LHCb-PUB-2014-039, 2014.
- [48] L. Anderlini *et al.*, The PIDCalib package, CERN, Report No. LHCb-PUB-2016-021, 2016.
- [49] A. Adare *et al.* (PHENIX Collaboration), Nuclear modification of ψ' , χ_c , and J/ψ production in $d + Au$ collisions at $\sqrt{s_{NN}} = 200$ GeV, *Phys. Rev. Lett.* **111**, 202301 (2013).
- [50] B. B. Abelev *et al.* (ALICE Collaboration), Suppression of $\psi(2S)$ production in p-Pb collisions at $\sqrt{s_{NN}} = 5.02$ TeV, *J. High Energy Phys.* **12** (2014) 073.
- [51] R. Aaij *et al.* (LHCb Collaboration), Study of $\psi(2S)$ production cross-sections and cold nuclear matter effects in pPb collisions at $\sqrt{s_{NN}} = 5$ TeV, *J. High Energy Phys.* **03** (2016) 133.
- [52] A. Adare *et al.* (PHENIX Collaboration), Measurement of the relative yields of $\psi(2S)$ to $\psi(1S)$ mesons produced at forward and backward rapidity in $p + p$, $p + Al$, $p + Au$, and $^3He + Au$ collisions at $\sqrt{s_{NN}} = 200$ GeV, *Phys. Rev. C* **95**, 034904 (2017).
- [53] A. M. Sirunyan *et al.* (CMS Collaboration), Measurement of prompt $\psi(2S)$ production cross sections in proton-lead and proton-proton collisions at $\sqrt{s_{NN}} = 5.02$ TeV, *Phys. Lett. B* **790**, 509 (2019).
- [54] S. Acharya *et al.* (ALICE Collaboration), Measurement of nuclear effects on $\psi(2S)$ production in p-Pb collisions at $\sqrt{s_{NN}} = 8.16$ TeV, *J. High Energy Phys.* **07** (2020) 237.
- [55] U. A. Acharya *et al.* (PHENIX Collaboration), Measurement of $\psi(2S)$ nuclear modification at backward and forward rapidity in $p + p$, $p + Al$, and $p + Au$ collisions at $\sqrt{s_{NN}} = 200$ GeV, *Phys. Rev. C* **105**, 064912 (2022).
- [56] R. Aaij *et al.* (LHCb Collaboration), Prompt and nonprompt $\psi(2S)$ production in pPb collisions at $\sqrt{s_{NN}} = 8.16$ TeV, *arXiv:2401.11342*.
- [57] B. Abelev *et al.* (ALICE Collaboration), Pseudorapidity density of charged particles in $p + Pb$ collisions at $\sqrt{s_{NN}} = 5.02$ TeV, *Phys. Rev. Lett.* **110**, 032301 (2013).
- [58] G. Aad *et al.* (ATLAS Collaboration), Measurement of the centrality dependence of the charged-particle pseudorapidity distribution in proton-lead collisions at $\sqrt{s_{NN}} = 5.02$ TeV with the ATLAS detector, *Eur. Phys. J. C* **76**, 199 (2016).

R. Aaij³⁵, A. S. W. Abdelmotteleb⁵⁴, C. Abellan Beteta⁴⁸, F. Abudinén⁵⁴, T. Ackernley⁵⁸, B. Adeva⁴⁴, M. Adinolfi⁵², P. Adlarson⁷⁸, C. Agapopoulou⁴⁶, C. A. Aidala⁷⁹, Z. Ajaltouni¹¹, S. Akar⁶³, K. Akiba³⁵, P. Albicocco²⁵, J. Albrecht¹⁷, F. Alessio⁴⁶, M. Alexander⁵⁷, A. Alfonso Alberro⁴³, Z. Aliouche⁶⁰

P. Alvarez Cartelle⁵³ R. Amalric¹⁵ S. Amato³ J. L. Amey⁵² Y. Amhis^{13,46} L. An⁶ L. Anderlini²⁴
M. Andersson⁴⁸ A. Andreianov⁴¹ P. Andreola⁴⁸ M. Andreotti²³ D. Andreou⁶⁶ A. A. Anelli²⁸ D. Ao⁷
F. Archilli^{34,u} M. Argenton²³ S. Arguedas Cuendis⁹ A. Artamonov⁹ M. Artuso⁶⁶ E. Aslanides¹²
M. Atzeni⁶² B. Audurier¹⁴ D. Bacher⁶¹ I. Bachiller Perea¹⁰ S. Bachmann¹⁹ M. Bachmayer⁴⁷ J. J. Back⁵⁴
A. Bailly-reyre¹⁵ P. Baladron Rodriguez⁴⁴ V. Balagura¹⁴ W. Baldini²³ J. Baptista de Souza Leite² M. Barbetti^{24,1}
I. R. Barbosa⁶⁷ R. J. Barlow⁶⁰ S. Barsuk¹³ W. Barter⁵⁶ M. Bartolini⁵³ F. Baryshnikov⁴¹ J. M. Basels¹⁶
G. Bassi^{32,4} B. Batsukh⁵ A. Battig¹⁷ A. Bay⁴⁷ A. Beck⁵⁴ M. Becker¹⁷ F. Bedeschi³² I. B. Bediaga²
A. Beiter⁶⁶ S. Belin⁴⁴ V. Bellee⁴⁸ K. Belous⁴¹ I. Belov²⁶ I. Belyaev⁴¹ G. Benane¹² G. Bencivenni²⁵
E. Ben-Haim¹⁵ A. Berezhnoy⁴¹ R. Bernet⁴⁸ S. Bernet Andres⁴² H. C. Bernstein⁶⁶ C. Bertella⁶⁰ A. Bertolin³⁰
C. Betancourt⁴⁸ F. Betti⁵⁶ J. Bex⁵³ Ia. Bezshyiko⁴⁸ J. Bhom³⁸ M. S. Bieker¹⁷ N. V. Biesuz²³ P. Billoir¹⁵
A. Biolchini³⁵ M. Birch⁵⁹ F. C. R. Bishop¹⁰ A. Bitadze⁶⁰ A. Bizzeti¹⁷ M. P. Blago⁵³ T. Blake⁵⁴ F. Blanc⁴⁷
J. E. Blank¹⁷ S. Blusk⁶⁶ D. Bobulski⁵⁷ V. Bocharnikov⁴¹ J. A. Boelhauve¹⁷ O. Boente Garcia¹⁴
T. Boettcher⁶³ A. Bohare⁵⁶ A. Boldyrev⁴¹ C. S. Bolognani⁷⁶ R. Bolzonella^{23,k} N. Bondar⁴¹ F. Borgato^{30,46}
S. Borghi⁶⁰ M. Borsato²⁸ J. T. Borsuk³⁸ S. A. Bouchiba⁴⁷ T. J. V. Bowcock⁵⁸ A. Boyer⁴⁶ C. Bozzi²³
M. J. Bradley⁵⁹ S. Braun⁶⁴ A. Brea Rodriguez⁴⁴ N. Breer¹⁷ J. Brodzicka³⁸ A. Brossa Gonzalo⁴⁴ J. Brown⁵⁸
D. Brundu²⁹ A. Buonaura⁴⁸ L. Buonincontri³⁰ A. T. Burke⁶⁰ C. Burr⁴⁶ A. Bursche⁶⁹ A. Butkevich⁴¹
J. S. Butter⁵³ J. Buytaert⁴⁶ W. Byczynski⁴⁶ S. Cadeddu²⁹ H. Cai⁷¹ R. Calabrese^{23,k} L. Calefice¹⁷ S. Cali²⁵
M. Calvi^{28,o} M. Calvo Gomez⁴² J. Cambon Bouzas⁴⁴ P. Campana²⁵ D. H. Campora Perez⁷⁶
A. F. Campoverde Quezada⁷ S. Capelli^{28,o} L. Capriotti²³ R. C. Caravaca-Mora⁹ A. Carbone^{22,1}
L. Carcedo Salgado⁴⁴ R. Cardinale^{26,m} A. Cardini²⁹ P. Carniti^{28,o} L. Carus¹⁹ A. Casais Vidal⁶² R. Caspary¹⁹
G. Casse⁵⁸ J. Castro Godinez⁹ M. Cattaneo⁴⁶ G. Cavallero²³ V. Cavallini^{23,k} S. Celani⁴⁷ J. Cerasoli¹²
D. Cervenkov⁶¹ S. Cesare^{27,n} A. J. Chadwick⁵⁸ I. Chahrouh⁷⁹ M. Charles¹⁵ Ph. Charpentier⁴⁶
C. A. Chavez Barajas⁵⁸ M. Chefdeville¹⁰ C. Chen¹² S. Chen⁵ A. Chernov³⁸ S. Chernyshenko⁵⁰
V. Chobanova^{44,y} S. Cholak⁴⁷ M. Chruszcz³⁸ A. Chubykin⁴¹ V. Chulikov⁴¹ P. Ciambrone²⁵ M. F. Cicala⁵⁴
X. Cid Vidal⁴⁴ G. Ciezarek⁴⁶ P. Cifra⁴⁶ P. E. L. Clarke⁵⁶ M. Clemencic⁴⁶ H. V. Cliff⁵³ J. Closier⁴⁶
J. L. Cobble Dick⁶⁰ C. Cocha Toapaxi¹⁹ V. Coco⁴⁶ J. Cogan¹² E. Cogneras¹¹ L. Cojocariu⁴⁰ P. Collins⁴⁶
T. Colombo⁴⁶ A. Comerma-Montells⁴³ L. Congedo²¹ A. Contu²⁹ N. Cooke⁵⁷ I. Corredoira⁴⁴ A. Correia¹⁵
G. Corti⁴⁶ J. J. Cottee Meldrum⁵² B. Couturier⁴⁶ D. C. Craik⁴⁸ M. Cruz Torres^{2,g} R. Currie⁵⁶ C. L. Da Silva⁶⁵
S. Dadabaev⁴¹ L. Dai⁶⁸ X. Dai⁶ E. Dall'Occo¹⁷ J. Dalseno⁴⁴ C. D'Ambrosio⁴⁶ J. Daniel¹¹ A. Danilina⁴¹
P. d'Argent²¹ A. Davidson⁵⁴ J. E. Davies⁶⁰ A. Davis⁶⁰ O. De Aguiar Francisco⁶⁰ C. De Angelis^{29,j}
J. de Boer³⁵ K. De Bruyn⁷⁵ S. De Capua⁶⁰ M. De Cian¹⁹ U. De Freitas Carneiro Da Graca^{2,c} E. De Lucia²⁵
J. M. De Miranda² L. De Paula³ M. De Serio^{21,h} D. De Simone⁴⁸ P. De Simone²⁵ F. De Vellis¹⁷
J. A. de Vries⁷⁶ F. Debernardis^{21,h} D. Decamp¹⁰ V. Dedu¹² L. Del Buono¹⁵ B. Delaney⁶² H.-P. Dembinski¹⁷
J. Deng⁸ V. Denysenko⁴⁸ O. Deschamps¹¹ F. Dettori^{29,j} B. Dey⁷⁴ P. Di Nezza²⁵ I. Diachkov⁴¹
S. Didenko⁴¹ S. Ding⁶⁶ V. Dobishuk⁵⁰ A. D. Docheva⁵⁷ A. Dolmatov⁴¹ C. Dong⁴ A. M. Donohoe²⁰
F. Dordei²⁹ A. C. dos Reis² L. Douglas⁵⁷ A. G. Downes¹⁰ W. Duan⁶⁹ P. Duda⁷⁷ M. W. Dudek³⁸
L. Dufour⁴⁶ V. Duk³¹ P. Durante⁴⁶ M. M. Duras⁷⁷ J. M. Durham⁶⁵ D. Dutta⁶⁰ A. Dziurda³⁸ A. Dzyuba⁴¹
S. Easo^{55,46} E. Eckstein⁷³ U. Egede¹ A. Egorychev⁴¹ V. Egorychev⁴¹ C. Eirea Orro⁴⁴ S. Eisenhardt⁵⁶
E. Ejopu⁶⁰ S. Ek-In⁴⁷ L. Eklund⁷⁸ M. Elashri⁶³ J. Ellbracht¹⁷ S. Ely⁵⁹ A. Ene⁴⁰ E. Epple⁶³ S. Escher¹⁶
J. Eschle⁴⁸ S. Esen⁴⁸ T. Evans⁶⁰ F. Fabiano^{29,46,j} L. N. Falcao² Y. Fan⁷ B. Fang^{71,13} L. Fantini^{31,q}
M. Faria⁴⁷ K. Farmer⁵⁶ D. Fazzini^{28,o} L. Felkowski⁷⁷ M. Feng^{5,7} M. Feo⁴⁶ M. Fernandez Gomez⁴⁴
A. D. Fernez⁶⁴ F. Ferrari²² F. Ferreira Rodrigues³ S. Ferreres Sole³⁵ M. Ferrillo⁴⁸ M. Ferro-Luzzi⁴⁶
S. Filippov⁴¹ R. A. Fini²¹ M. Fiorini^{23,k} M. Firlej³⁷ K. M. Fischer⁶¹ D. S. Fitzgerald⁷⁹ C. Fitzpatrick⁶⁰
T. Fiutowski³⁷ F. Fleuret¹⁴ M. Fontana²² F. Fontanelli^{26,m} L. F. Foreman⁶⁰ R. Forty⁴⁶ D. Foulds-Holt⁵³
M. Franco Sevilla⁶⁴ M. Frank⁴⁶ E. Franzoso^{23,k} G. Frau¹⁹ C. Frei⁴⁶ D. A. Friday⁶⁰ L. Frontini^{27,n} J. Fu⁷
Q. Fuehring¹⁷ Y. Fujii¹ T. Fulghesu¹⁵ E. Gabriel³⁵ G. Galati^{21,h} M. D. Galati³⁵ A. Gallas Torreira⁴⁴
D. Galli^{22,1} S. Gambetta^{56,46} M. Gandelman³ P. Gandini²⁷ H. Gao⁷ R. Gao⁶¹ Y. Gao⁸ Y. Gao⁶ Y. Gao⁸
M. Garau^{29,j} L. M. Garcia Martin⁴⁷ P. Garcia Moreno⁴³ J. Garcia Pardiñas⁴⁶ B. Garcia Plana⁴⁴ K. G. Garg⁸
L. Garrido⁴³ C. Gaspar⁴⁶ R. E. Geertsema³⁵ L. L. Gerken¹⁷ E. Gersabeck⁶⁰ M. Gersabeck⁶⁰ T. Gershon⁵⁴

Z. Ghorbanimoghaddam,⁵² L. Giambastiani,³⁰ F. I. Giasemis,^{15,e} V. Gibson,⁵³ H. K. Gienza,³⁹ A. L. Gilman,⁶¹ M. Giovannetti,²⁵ A. Gioventù,⁴³ P. Gironella Gironell,⁴³ C. Giugliano,^{23,k} M. A. Giza,³⁸ E. L. Gkoukousis,⁵⁹ F. C. Glaser,^{13,19} V. V. Gligorov,¹⁵ C. Göbel,⁶⁷ E. Golobardes,⁴² D. Golubkov,⁴¹ A. Golutvin,^{59,41,46} A. Gomes,^{2b,a} S. Gomez Fernandez,⁴³ F. Goncalves Abrantes,⁶¹ M. Goncerz,³⁸ G. Gong,⁴ J. A. Gooding,¹⁷ I. V. Gorelov,⁴¹ C. Gotti,²⁸ J. P. Grabowski,⁷³ L. A. Granado Cardoso,⁴⁶ E. Graugés,⁴³ E. Graverini,⁴⁷ L. Grazette,⁵⁴ G. Graziani, A. T. Grecu,⁴⁰ L. M. Greeven,³⁵ N. A. Grieser,⁶³ L. Grillo,⁵⁷ S. Gromov,⁴¹ C. Gu,¹⁴ M. Guarise,²³ M. Guittiere,¹³ V. Guliaeva,⁴¹ P. A. Günther,¹⁹ A.-K. Guseinov,⁴¹ E. Gushchin,⁴¹ Y. Guz,^{6,41,46} T. Gys,⁴⁶ T. Hadavizadeh,¹ C. Hadjivasiliou,⁶⁴ G. Haefeli,⁴⁷ C. Haen,⁴⁶ J. Haimberger,⁴⁶ M. Hajheidari,⁴⁶ T. Halewood-leagas,⁵⁸ M. M. Halvorsen,⁴⁶ P. M. Hamilton,⁶⁴ J. Hammerich,⁵⁸ Q. Han,⁸ X. Han,¹⁹ S. Hansmann-Menzemer,¹⁹ L. Hao,⁷ N. Harnew,⁶¹ T. Harrison,⁵⁸ M. Hartmann,¹³ C. Hasse,⁴⁶ J. He,^{7,d} K. Heijhoff,³⁵ F. Hemmer,⁴⁶ C. Henderson,⁶³ R. D. L. Henderson,^{1,54} A. M. Hennequin,⁴⁶ K. Hennessy,⁵⁸ L. Henry,⁴⁷ J. Herd,⁵⁹ J. Heuel,¹⁶ A. Hicheur,³ D. Hill,⁴⁷ S. E. Hollitt,¹⁷ J. Horswill,⁶⁰ R. Hou,⁸ Y. Hou,¹⁰ N. Howarth,⁵⁸ J. Hu,¹⁹ J. Hu,⁶⁹ W. Hu,⁶ X. Hu,⁴ W. Huang,⁷ W. Hulsbergen,³⁵ R. J. Hunter,⁵⁴ M. Hushchyn,⁴¹ D. Hutchcroft,⁵⁸ M. Idzik,³⁷ D. Ilin,⁴¹ P. Ilten,⁶³ A. Inglessi,⁴¹ A. Iniukhin,⁴¹ A. Ishteev,⁴¹ K. Ivshin,⁴¹ R. Jacobsson,⁴⁶ H. Jage,¹⁶ S. J. Jaimes Elles,^{45,72} S. Jakobsen,⁴⁶ E. Jans,³⁵ B. K. Jashal,⁴⁵ A. Jawahery,⁶⁴ V. Jevtic,¹⁷ E. Jiang,⁶⁴ X. Jiang,^{5,7} Y. Jiang,⁷ Y. J. Jiang,⁶ M. John,⁶¹ D. Johnson,⁵¹ C. R. Jones,⁵³ T. P. Jones,⁵⁴ S. Joshi,³⁹ B. Jost,⁴⁶ N. Jurik,⁴⁶ I. Juszcak,³⁸ D. Kaminaris,⁴⁷ S. Kandybei,⁴⁹ Y. Kang,⁴ M. Karacson,⁴⁶ D. Karpenkov,⁴¹ M. Karpov,⁴¹ A. M. Kauniskangas,⁴⁷ J. W. Kautz,⁶³ F. Keizer,⁴⁶ D. M. Keller,⁶⁶ M. Kenzie,⁵³ T. Ketel,³⁵ B. Khanji,⁶⁶ A. Kharisova,⁴¹ S. Kholodenko,³² G. Khreich,¹³ T. Kim,¹⁶ V. S. Kirsebom,⁴⁷ O. Kitouni,⁶² S. Klaver,³⁶ N. Kleijne,^{32,r} K. Klimaszewski,³⁹ M. R. Kmiec,³⁹ S. Koliiev,⁵⁰ L. Kolk,¹⁷ A. Konoplyannikov,⁴¹ P. Kopciwicz,^{37,46} P. Koppenburg,³⁵ M. Korolev,⁴¹ I. Kostiuk,³⁵ O. Kot,⁵⁰ S. Kotriakhova, A. Kozachuk,⁴¹ P. Kravchenko,⁴¹ L. Kravchuk,⁴¹ M. Kreps,⁵⁴ S. Kretschmar,¹⁶ P. Krokovny,⁴¹ W. Krupa,⁶⁶ W. Krzemien,³⁹ J. Kubat,¹⁹ S. Kubis,⁷⁷ W. Kucewicz,³⁸ M. Kucharczyk,³⁸ V. Kudryavtsev,⁴¹ E. Kulikova,⁴¹ A. Kupsc,⁷⁸ B. K. Kutsenko,¹² D. Lacarrere,⁴⁶ G. Lafferty,⁶⁰ A. Lai,²⁹ A. Lampis,²⁹ D. Lancierini,⁴⁸ C. Landesa Gomez,⁴⁴ J. J. Lane,¹ R. Lane,⁵² C. Langenbruch,¹⁹ J. Langer,¹⁷ O. Lantwin,⁴¹ T. Latham,⁵⁴ F. Lazzari,^{32,s} C. Lazzeroni,⁵¹ R. Le Gac,¹² S. H. Lee,⁷⁹ R. Lefèvre,¹¹ A. Leflat,⁴¹ S. Legotin,⁴¹ M. Lehuraux,⁵⁴ O. Leroy,¹² T. Lesiak,³⁸ B. Leverington,¹⁹ A. Li,⁴ H. Li,⁶⁹ K. Li,⁸ L. Li,⁶⁰ P. Li,⁴⁶ P.-R. Li,⁷⁰ S. Li,⁸ T. Li,⁵ T. Li,⁶⁹ Y. Li,⁸ Y. Li,⁵ Z. Li,⁶⁶ Z. Lian,⁴ X. Liang,⁶⁶ C. Lin,⁷ T. Lin,⁵⁵ R. Lindner,⁴⁶ V. Lisovskyi,⁴⁷ R. Litvinov,^{29,j} G. Liu,⁶⁹ H. Liu,⁷ K. Liu,⁷⁰ Q. Liu,⁷ S. Liu,^{5,7} Y. Liu,⁵⁶ Y. Liu,⁷⁰ Y. L. Liu,⁵⁹ A. Lobo Salvia,⁴³ A. Loi,²⁹ J. Lomba Castro,⁴⁴ T. Long,⁵³ J. H. Lopes,³ A. Lopez Huertas,⁴³ S. López Soliño,⁴⁴ G. H. Lovell,⁵³ C. Lucarelli,^{24,1} D. Lucchesi,^{30,p} S. Luchuk,⁴¹ M. Lucio Martinez,⁷⁶ V. Lukashenko,^{35,50} Y. Luo,⁴ A. Lupato,³⁰ E. Luppi,^{23,k} K. Lynch,²⁰ X.-R. Lyu,⁷ G. M. Ma,⁴ R. Ma,⁷ S. Maccolini,¹⁷ F. Machefer,¹³ F. Maciuc,⁴⁰ I. Mackay,⁶¹ L. R. Madhan Mohan,⁵³ M. M. Madurai,⁵¹ A. Maevskiy,⁴¹ D. Magdalinski,³⁵ D. Maisuzenko,⁴¹ M. W. Majewski,³⁷ J. J. Malczewski,³⁸ S. Malde,⁶¹ B. Malecki,^{38,46} L. Malentacca,⁴⁶ A. Malinin,⁴¹ T. Maltsev,⁴¹ G. Manca,^{29,j} G. Mancinelli,¹² C. Mancuso,^{27,13,n} R. Manera Escalero,⁴³ D. Manuzzi,²² D. Marangotto,^{27,n} J. F. Marchand,¹⁰ R. Marchewski,⁴⁷ U. Marconi,²² S. Mariani,⁴⁶ C. Marin Benito,^{43,46} J. Marks,¹⁹ A. M. Marshall,⁵² P. J. Marshall,⁵⁸ G. Martelli,^{31,q} G. Martellotti,³³ L. Martinazzoli,⁴⁶ M. Martinelli,^{28,o} D. Martinez Santos,⁴⁴ F. Martinez Vidal,⁴⁵ A. Massafferri,² M. Materok,¹⁶ R. Matev,⁴⁶ A. Mathad,⁴⁸ V. Matiunin,⁴¹ C. Matteuzzi,⁶⁶ K. R. Mattioli,¹⁴ A. Mauri,⁵⁹ E. Maurice,¹⁴ J. Mauricio,⁴³ P. Mayencourt,⁴⁷ M. Mazurek,⁴⁶ M. McCann,⁵⁹ L. McConnell,²⁰ T. H. McGrath,⁶⁰ N. T. McHugh,⁵⁷ A. McNab,⁶⁰ R. McNulty,²⁰ B. Meadows,⁶³ G. Meier,¹⁷ D. Melnychuk,³⁹ M. Merk,^{35,76} A. Merli,^{27,n} L. Meyer Garcia,³ D. Miao,^{5,7} H. Miao,⁷ M. Mikhasenko,^{73,f} D. A. Milanese,⁷² A. Minotti,^{28,o} E. Minucci,⁶⁶ T. Miralles,¹¹ S. E. Mitchell,⁵⁶ B. Mitreska,¹⁷ D. S. Mitzel,¹⁷ A. Modak,⁵⁵ A. Mödden,¹⁷ R. A. Mohammed,⁶¹ R. D. Moise,¹⁶ S. Mokhnenko,⁴¹ T. Mombächer,⁴⁶ M. Monk,^{54,1} I. A. Monroy,⁷² S. Monteil,¹¹ A. Morcillo Gomez,⁴⁴ G. Morello,²⁵ M. J. Morello,^{32,r} M. P. Morgenthaler,¹⁹ J. Moron,³⁷ A. B. Morris,⁴⁶ A. G. Morris,¹² R. Mountain,⁶⁶ H. Mu,⁴ Z. M. Mu,⁶ E. Muhammad,⁵⁴ F. Muheim,⁵⁶ M. Mulder,⁷⁵ K. Müller,⁴⁸ F. Muñoz-Rojas,⁹ R. Murta,⁵⁹ P. Naik,⁵⁸ T. Nakada,⁴⁷ R. Nandakumar,⁵⁵ T. Nanut,⁴⁶ I. Nasteva,³ M. Needham,⁵⁶ N. Neri,^{27,n} S. Neubert,⁷³ N. Neufeld,⁴⁶ P. Neustroev,⁴¹ R. Newcombe,⁵⁹ J. Nicolini,^{17,13} D. Nicotra,⁷⁶ E. M. Niel,⁴⁷ N. Nikitin,⁴¹ P. Nogga,⁷³ N. S. Nolte,⁶² C. Normand,^{10,29,j}

J. Novoa Fernandez⁴⁴ G. Nowak⁶³ C. Nunez⁷⁹ H. N. Nur⁵⁷ A. Oblakowska-Mucha³⁷ V. Obraztsov⁴¹
T. Oeser¹⁶ S. Okamura^{23,46,k} A. Okhotnikov, R. Oldeman^{29,j} F. Oliva⁵⁶ M. Olocco¹⁷ C. J. G. Onderwater⁷⁶
R. H. O'Neil⁵⁶ J. M. Otalora Goicochea³ T. Ovsiannikova⁴¹ P. Owen⁴⁸ A. Oyanguren⁴⁵ O. Ozelik⁵⁶
K. O. Padeken⁷³ B. Pagare⁵⁴ P. R. Pais¹⁹ T. Pajero⁶¹ A. Palano²¹ M. Palutan²⁵ G. Panshin⁴¹ L. Paolucci⁵⁴
A. Papanestis⁵⁵ M. Pappagallo^{21,h} L. L. Pappalardo^{23,k} C. Pappenheimer⁶³ C. Parkes⁶⁰ B. Passalacqua^{23,k}
G. Passaleva²⁴ D. Passaro³² A. Pastore²¹ M. Patel⁵⁹ J. Patoc⁶¹ C. Patrignani^{22,i} C. J. Pawley⁷⁶
A. Pellegrino³⁵ M. Pepe Altarelli²⁵ S. Perazzini²² D. Pereima⁴¹ A. Pereiro Castro⁴⁴ P. Perret¹¹ A. Perro⁴⁶
K. Petridis⁵² A. Petrolini^{26,m} S. Petrucci⁵⁶ H. Pham⁶⁶ L. Pica³² M. Piccini³¹ B. Pietrzyk¹⁰ G. Pietrzyk¹³
D. Pinci³³ F. Pisani⁴⁶ M. Pizzichemi^{28,o} V. Placinta⁴⁰ M. Plo Casasus⁴⁴ F. Polci^{15,46} M. Poli Lener²⁵
A. Poluektov¹² N. Polukhina⁴¹ I. Polyakov⁴⁶ E. Polycarpo³ S. Ponce⁴⁶ D. Popov⁷ S. Poslavskii⁴¹
K. Prasanth³⁸ L. Promberger¹⁹ C. Prouve⁴⁴ V. Pugatch⁵⁰ V. Puill¹³ G. Punzi^{32,s} H. R. Qi⁴ W. Qian⁷
N. Qin⁴ S. Qu⁴ R. Quagliani⁴⁷ R. I. Rabadan Trejo⁵⁴ B. Rachwal³⁷ J. H. Rademacker⁵² M. Rama³²
M. Ramírez García⁷⁹ M. Ramos Pernas⁵⁴ M. S. Rangel³ F. Ratnikov⁴¹ G. Raven³⁶ M. Rebollo De Miguel⁴⁵
F. Redi⁴⁶ J. Reich⁵² F. Reiss⁶⁰ Z. Ren⁷ P. K. Resmi⁶¹ R. Ribatti^{32,r} G. R. Ricart^{14,80} D. Ricciardi³²
S. Ricciardi⁵⁵ K. Richardson⁶² M. Richardson-Slipper⁵⁶ K. Rinnert⁵⁸ P. Robbe¹³ G. Robertson⁵⁷
E. Rodrigues^{58,46} E. Rodriguez Fernandez⁴⁴ J. A. Rodriguez Lopez⁷² E. Rodriguez Rodriguez⁴⁴ A. Rogovskiy⁵⁵
D. L. Rolf⁴⁶ A. Rollings⁶¹ P. Roloff⁴⁶ V. Romanovskiy⁴¹ M. Romero Lamas⁴⁴ A. Romero Vidal⁴⁴
G. Romolini²³ F. Ronchetti⁴⁷ M. Rotondo²⁵ S. R. Roy¹⁹ M. S. Rudolph⁶⁶ T. Ruf⁴⁶ M. Ruiz Diaz¹⁹
R. A. Ruiz Fernandez⁴⁴ J. Ruiz Vidal^{78,z} A. Ryzhikov⁴¹ J. Ryzka³⁷ J. J. Saborido Silva⁴⁴ R. Sadek¹⁴
N. Sagidova⁴¹ N. Sahoo⁵¹ B. Saitta^{29,j} M. Salomoni^{28,o} C. Sanchez Gras³⁵ I. Sanderswood⁴⁵
R. Santacesaria³³ C. Santamarina Rios⁴⁴ M. Santimaria²⁵ L. Santoro² E. Santovetti³⁴ A. Saputi^{23,46}
D. Saranin⁴¹ G. Sarpis⁵⁶ M. Sarpis⁷³ A. Sarti³³ C. Satriano^{33,t} A. Satta³⁴ M. Saur⁶ D. Savrina⁴¹
H. Sazak¹¹ L. G. Scantlebury Smead⁶¹ A. Scarabotto¹⁵ S. Schael¹⁶ S. Scherl⁵⁸ A. M. Schertz⁷⁴
M. Schiller⁵⁷ H. Schindler⁴⁶ M. Schmelling¹⁸ B. Schmidt⁴⁶ S. Schmitt¹⁶ H. Schmitz⁷³ O. Schneider⁴⁷
A. Schopper⁴⁶ N. Schulte¹⁷ S. Schulte⁴⁷ M. H. Schune¹³ R. Schwemmer⁴⁶ G. Schwering¹⁶ B. Sciascia²⁵
A. Sciuccati⁴⁶ S. Sellam⁴⁴ A. Semennikov⁴¹ M. Senghi Soares³⁶ A. Sergi^{26,m} N. Serra^{48,46} L. Sestini³⁰
A. Seuthe¹⁷ Y. Shang⁶ D. M. Shangase⁷⁹ M. Shapkin⁴¹ I. Shchemerov⁴¹ L. Shchutska⁴⁷ T. Shears⁵⁸
L. Shekhtman⁴¹ Z. Shen⁶ S. Sheng^{5,7} V. Shevchenko⁴¹ B. Shi⁷ E. B. Shields^{28,o} Y. Shimizu¹³
E. Shmanin⁴¹ R. Shorkin⁴¹ J. D. Shupperd⁶⁶ R. Silva Coutinho⁶⁶ G. Simi³⁰ S. Simone^{21,h} N. Skidmore⁶⁰
R. Skuza¹⁹ T. Skwarnicki⁶⁶ M. W. Slater⁵¹ J. C. Smallwood⁶¹ E. Smith⁶² K. Smith⁶⁵ M. Smith⁵⁹
A. Snoch³⁵ L. Soares Lavra⁵⁶ M. D. Sokoloff⁶³ F. J. P. Soler⁵⁷ A. Solomin^{41,52} A. Solovev⁴¹ I. Solovyev⁴¹
R. Song¹ Y. Song⁴⁷ Y. Song⁴ Y. S. Song⁶ F. L. Souza De Almeida⁶⁶ B. Souza De Paula³
E. Spadaro Norella^{27,n} E. Spedicato²² J. G. Speer¹⁷ E. Spiridenkov⁴¹ P. Spradlin⁵⁷ V. Srisakaran⁴⁶ F. Stagni⁴⁶
M. Stahl⁴⁶ S. Stahl⁴⁶ S. Stanislaus⁶¹ E. N. Stein⁴⁶ O. Steinkamp⁴⁸ O. Stenyakin⁴¹ H. Stevens¹⁷
D. Strelakina⁴¹ Y. Su⁷ F. Suljik⁶¹ J. Sun²⁹ L. Sun⁷¹ Y. Sun⁶⁴ P. N. Swallow⁵¹ K. Swientek³⁷
F. Swystun⁵⁴ A. Szabelski³⁹ T. Szumlak³⁷ M. Szymanski⁴⁶ Y. Tan⁴ S. Taneja⁶⁰ M. D. Tat⁶¹ A. Terentev⁴⁸
F. Terzuoli^{32,v} F. Teubert⁴⁶ E. Thomas⁴⁶ D. J. D. Thompson⁵¹ H. Tilquin⁵⁹ V. Tisserand¹¹ S. T'Jampens¹⁰
M. Tobin⁵ L. Tomassetti^{23,k} G. Tonani^{27,n} X. Tong⁶ D. Torres Machado² L. Toscano¹⁷ D. Y. Tou⁴
C. Trippel⁴² G. Tuci¹⁹ N. Tuning³⁵ L. H. Uecker¹⁹ A. Ukleja³⁷ D. J. Unverzagt¹⁹ E. Ursov⁴¹ A. Usachov³⁶
A. Ustyuzhanin⁴¹ U. Uwer¹⁹ V. Vagnoni²² A. Valassi⁴⁶ G. Valenti²² N. Valls Canudas⁴² H. Van Hecke⁶⁵
E. van Herwijnen⁵⁹ C. B. Van Hulse^{44,x} R. Van Laak⁴⁷ M. van Veghel³⁵ R. Vazquez Gomez⁴³
P. Vazquez Regueiro⁴⁴ C. Vázquez Sierra⁴⁴ S. Vecchi²³ J. J. Velthuis⁵² M. Veltri^{24,w} A. Venkateswaran⁴⁷
M. Vesterinen⁵⁴ D. Vieira⁶³ M. Vieites Diaz⁴⁶ X. Vilasis-Cardona⁴² E. Vilella Figueras⁵⁸ A. Villa²²
P. Vincent¹⁵ F. C. Volle¹³ D. vom Bruch¹² V. Vorobyev⁴¹ N. Voropaev⁴¹ K. Vos⁷⁶ G. Vouters¹⁰ C. Vrahas⁵⁶
J. Walsh³² E. J. Walton¹ G. Wan⁶ C. Wang¹⁹ G. Wang⁸ J. Wang⁶ J. Wang⁵ J. Wang⁴ J. Wang⁷¹
M. Wang²⁷ N. W. Wang⁷ R. Wang⁵² X. Wang⁶⁹ X. W. Wang⁵⁹ Y. Wang⁸ Z. Wang¹³ Z. Wang⁴
Z. Wang⁷ J. A. Ward^{54,1} N. K. Watson⁵¹ D. Websdale⁵⁹ Y. Wei⁶ B. D. C. Westhenry⁵² D. J. White⁶⁰
M. Whitehead⁵⁷ A. R. Wiederhold⁵⁴ D. Wiedner¹⁷ G. Wilkinson⁶¹ M. K. Wilkinson⁶³ M. Williams⁶²
M. R. J. Williams⁵⁶ R. Williams⁵³ F. F. Wilson⁵⁵ W. Wislicki³⁹ M. Witek³⁸ L. Witola¹⁹ C. P. Wong⁶⁵

G. Wormser¹³, S. A. Wotton⁵³, H. Wu⁶⁶, J. Wu⁸, Y. Wu⁶, K. Wyllie⁴⁶, S. Xian⁶⁹, Z. Xiang⁵, Y. Xie⁸, A. Xu³², J. Xu⁷, L. Xu⁴, L. Xu⁴, M. Xu⁵⁴, Z. Xu¹¹, Z. Xu⁷, Z. Xu⁵, D. Yang⁴, S. Yang⁷, X. Yang⁶, Y. Yang²⁶, Z. Yang⁶, Z. Yang⁶⁴, V. Yeroshenko¹³, H. Yeung⁶⁰, H. Yin⁸, C. Y. Yu⁶, J. Yu⁶⁸, X. Yuan⁵, E. Zaffaroni⁴⁷, M. Zavertyaev¹⁸, M. Zdybal³⁸, M. Zeng⁴, C. Zhang⁶, D. Zhang⁸, J. Zhang⁷, L. Zhang⁴, S. Zhang⁶⁸, S. Zhang⁶, Y. Zhang⁶, Y. Zhang⁶¹, Y. Z. Zhang⁴, Y. Zhao¹⁹, A. Zharkova⁴¹, A. Zhelezov¹⁹, X. Z. Zheng⁴, Y. Zheng⁷, T. Zhou⁶, X. Zhou⁸, Y. Zhou⁷, V. Zhovkovska⁵⁴, L. Z. Zhu⁷, X. Zhu⁴, X. Zhu⁸, Z. Zhu⁷, V. Zhukov^{16,41}, J. Zhuo⁴⁵, Q. Zou^{5,7}, D. Zuliani³⁰ and G. Zunica⁶⁰

(LHCb Collaboration)

¹*School of Physics and Astronomy, Monash University, Melbourne, Australia*

²*Centro Brasileiro de Pesquisas Físicas (CBPF), Rio de Janeiro, Brazil*

³*Universidade Federal do Rio de Janeiro (UFRJ), Rio de Janeiro, Brazil*

⁴*Center for High Energy Physics, Tsinghua University, Beijing, China*

⁵*Institute Of High Energy Physics (IHEP), Beijing, China*

⁶*School of Physics State Key Laboratory of Nuclear Physics and Technology, Peking University, Beijing, China*

⁷*University of Chinese Academy of Sciences, Beijing, China*

⁸*Institute of Particle Physics, Central China Normal University, Wuhan, Hubei, China*

⁹*Consejo Nacional de Rectores (CONARE), San Jose, Costa Rica*

¹⁰*Université Savoie Mont Blanc, CNRS, IN2P3-LAPP, Annecy, France*

¹¹*Université Clermont Auvergne, CNRS/IN2P3, LPC, Clermont-Ferrand, France*

¹²*Aix Marseille Univ, CNRS/IN2P3, CPPM, Marseille, France*

¹³*Université Paris-Saclay, CNRS/IN2P3, IJCLab, Orsay, France*

¹⁴*Laboratoire Leprince-Ringuet, CNRS/IN2P3, Ecole Polytechnique, Institut Polytechnique de Paris, Palaiseau, France*

¹⁵*LPNHE, Sorbonne Université, Paris Diderot Sorbonne Paris Cité, CNRS/IN2P3, Paris, France*

¹⁶*I. Physikalisches Institut, RWTH Aachen University, Aachen, Germany*

¹⁷*Fakultät Physik, Technische Universität Dortmund, Dortmund, Germany*

¹⁸*Max-Planck-Institut für Kernphysik (MPIK), Heidelberg, Germany*

¹⁹*Physikalisches Institut, Ruprecht-Karls-Universität Heidelberg, Heidelberg, Germany*

²⁰*School of Physics, University College Dublin, Dublin, Ireland*

²¹*INFN Sezione di Bari, Bari, Italy*

²²*INFN Sezione di Bologna, Bologna, Italy*

²³*INFN Sezione di Ferrara, Ferrara, Italy*

²⁴*INFN Sezione di Firenze, Firenze, Italy*

²⁵*INFN Laboratori Nazionali di Frascati, Frascati, Italy*

²⁶*INFN Sezione di Genova, Genova, Italy*

²⁷*INFN Sezione di Milano, Milano, Italy*

²⁸*INFN Sezione di Milano-Bicocca, Milano, Italy*

²⁹*INFN Sezione di Cagliari, Monserrato, Italy*

³⁰*Università degli Studi di Padova, Università e INFN, Padova, Padova, Italy*

³¹*INFN Sezione di Perugia, Perugia, Italy*

³²*INFN Sezione di Pisa, Pisa, Italy*

³³*INFN Sezione di Roma La Sapienza, Roma, Italy*

³⁴*INFN Sezione di Roma Tor Vergata, Roma, Italy*

³⁵*Nikhef National Institute for Subatomic Physics, Amsterdam, Netherlands*

³⁶*Nikhef National Institute for Subatomic Physics and VU University Amsterdam, Amsterdam, Netherlands*

³⁷*AGH—University of Science and Technology, Faculty of Physics and Applied Computer Science, Kraków, Poland*

³⁸*Henryk Niewodniczanski Institute of Nuclear Physics Polish Academy of Sciences, Kraków, Poland*

³⁹*National Center for Nuclear Research (NCBJ), Warsaw, Poland*

⁴⁰*Horia Hulubei National Institute of Physics and Nuclear Engineering, Bucharest-Magurele, Romania*

⁴¹*Affiliated with an institute covered by a cooperation agreement with CERN*

⁴²*DS4DS, La Salle, Universitat Ramon Llull, Barcelona, Spain*

⁴³*ICCUB, Universitat de Barcelona, Barcelona, Spain*

⁴⁴*Instituto Galego de Física de Altas Enerxías (IGFAE), Universidade de Santiago de Compostela, Santiago de Compostela, Spain*

⁴⁵*Instituto de Física Corpuscular, Centro Mixto Universidad de Valencia—CSIC, Valencia, Spain*

⁴⁶*European Organization for Nuclear Research (CERN), Geneva, Switzerland*

⁴⁷*Institute of Physics, Ecole Polytechnique Fédérale de Lausanne (EPFL), Lausanne, Switzerland*

- ⁴⁸*Physik-Institut, Universität Zürich, Zürich, Switzerland*
- ⁴⁹*NSC Kharkiv Institute of Physics and Technology (NSC KIPT), Kharkiv, Ukraine*
- ⁵⁰*Institute for Nuclear Research of the National Academy of Sciences (KINR), Kyiv, Ukraine*
- ⁵¹*University of Birmingham, Birmingham, United Kingdom*
- ⁵²*H.H. Wills Physics Laboratory, University of Bristol, Bristol, United Kingdom*
- ⁵³*Cavendish Laboratory, University of Cambridge, Cambridge, United Kingdom*
- ⁵⁴*Department of Physics, University of Warwick, Coventry, United Kingdom*
- ⁵⁵*STFC Rutherford Appleton Laboratory, Didcot, United Kingdom*
- ⁵⁶*School of Physics and Astronomy, University of Edinburgh, Edinburgh, United Kingdom*
- ⁵⁷*School of Physics and Astronomy, University of Glasgow, Glasgow, United Kingdom*
- ⁵⁸*Oliver Lodge Laboratory, University of Liverpool, Liverpool, United Kingdom*
- ⁵⁹*Imperial College London, London, United Kingdom*
- ⁶⁰*Department of Physics and Astronomy, University of Manchester, Manchester, United Kingdom*
- ⁶¹*Department of Physics, University of Oxford, Oxford, United Kingdom*
- ⁶²*Massachusetts Institute of Technology, Cambridge, Massachusetts, USA*
- ⁶³*University of Cincinnati, Cincinnati, Ohio, USA*
- ⁶⁴*University of Maryland, College Park, Maryland, USA*
- ⁶⁵*Los Alamos National Laboratory (LANL), Los Alamos, New Mexico, USA*
- ⁶⁶*Syracuse University, Syracuse, New York, USA*
- ⁶⁷*Pontifícia Universidade Católica do Rio de Janeiro (PUC-Rio), Rio de Janeiro, Brazil, associated to Universidade Federal do Rio de Janeiro (UFRJ), Rio de Janeiro, Brazil*
- ⁶⁸*Physics and Micro Electronic College, Hunan University, Changsha City, China, associated to Institute of Particle Physics, Central China Normal University, Wuhan, Hubei, China*
- ⁶⁹*Guangdong Provincial Key Laboratory of Nuclear Science, Guangdong-Hong Kong Joint Laboratory of Quantum Matter, Institute of Quantum Matter, South China Normal University, Guangzhou, China, associated to Center for High Energy Physics, Tsinghua University, Beijing, China*
- ⁷⁰*Lanzhou University, Lanzhou, China, associated to Institute Of High Energy Physics (IHEP), Beijing, China*
- ⁷¹*School of Physics and Technology, Wuhan University, Wuhan, China, associated to Center for High Energy Physics, Tsinghua University, Beijing, China*
- ⁷²*Departamento de Física, Universidad Nacional de Colombia, Bogota, Colombia, associated to LPNHE, Sorbonne Université, Paris Diderot Sorbonne Paris Cité, CNRS/IN2P3, Paris, France*
- ⁷³*Universität Bonn—Helmholtz-Institut für Strahlen und Kernphysik, Bonn, Germany, associated to Physikalisches Institut, Ruprecht-Karls-Universität Heidelberg, Heidelberg, Germany*
- ⁷⁴*Eotvos Lorand University, Budapest, Hungary, associated to European Organization for Nuclear Research (CERN), Geneva, Switzerland*
- ⁷⁵*Van Swinderen Institute, University of Groningen, Groningen, Netherlands, associated to Nikhef National Institute for Subatomic Physics, Amsterdam, Netherlands*
- ⁷⁶*Universiteit Maastricht, Maastricht, Netherlands, associated to Nikhef National Institute for Subatomic Physics, Amsterdam, Netherlands*
- ⁷⁷*Tadeusz Kosciuszko Cracow University of Technology, Cracow, Poland, associated to Henryk Niewodniczanski Institute of Nuclear Physics Polish Academy of Sciences, Kraków, Poland*
- ⁷⁸*Department of Physics and Astronomy, Uppsala University, Uppsala, Sweden, associated to School of Physics and Astronomy, University of Glasgow, Glasgow, United Kingdom*
- ⁷⁹*University of Michigan, Ann Arbor, Michigan, USA, associated to Syracuse University, Syracuse, New York, USA*
- ⁸⁰*Departement de Physique Nucleaire (SPhN), Gif-Sur-Yvette, France*

^aDeceased.

^bUniversidade de Brasília, Brasília, Brazil.

^cCentro Federal de Educação Tecnológica Celso Suckow da Fonseca, Rio De Janeiro, Brazil.

^dHangzhou Institute for Advanced Study, UCAS, Hangzhou, China.

^eLIP6, Sorbonne Université, Paris, France.

^fExcellence Cluster ORIGINS, Munich, Germany.

^gUniversidad Nacional Autónoma de Honduras, Tegucigalpa, Honduras.

^hUniversità di Bari, Bari, Italy.

ⁱUniversità di Bologna, Bologna, Italy.

^jUniversità di Cagliari, Cagliari, Italy.

^kUniversità di Ferrara, Ferrara, Italy.

^lUniversità di Firenze, Firenze, Italy.

^mUniversità di Genova, Genova, Italy.

ⁿUniversità degli Studi di Milano, Milano, Italy.

^oUniversità di Milano Bicocca, Milano, Italy.

^pUniversità di Padova, Padova, Italy.

^qUniversità di Perugia, Perugia, Italy.

^rScuola Normale Superiore, Pisa, Italy.

^sUniversità di Pisa, Pisa, Italy.

^tUniversità della Basilicata, Potenza, Italy.

^uUniversità di Roma Tor Vergata, Roma, Italy.

^vUniversità di Siena, Siena, Italy.

^wUniversità di Urbino, Urbino, Italy.

^xUniversidad de Alcalá, Alcalá de Henares, Spain.

^yUniversidade da Coruña, Coruña, Spain.

^zDepartment of Physics/Division of Particle Physics, Lund, Sweden.